

Activated Tissue-Resident Mesenchymal Stromal Cells Regulate Natural Killer Cell Immune and Tissue-Regenerative Function

Robert Michael Petri,¹ Alexander Hackel,¹ Katrin Hahnel,¹ Claudia Alexandra Dumitru,¹ Kirsten Bruderek,¹ Stefanie B. Flohe,² Annette Paschen,³ Stephan Lang,¹ and Sven Brandau^{1,*}

¹Department of Otorhinolaryngology, University Hospital Essen, University of Duisburg-Essen, Essen 45147, Germany

²Department of Orthopedics and Trauma Surgery, University Hospital Essen, University of Duisburg-Essen, Essen 45147, Germany

³Department of Dermatology, University Hospital Essen, University of Duisburg-Essen, Essen 45147, Germany

*Correspondence: sven.brandau@uk-essen.de

<http://dx.doi.org/10.1016/j.stemcr.2017.06.020>

SUMMARY

The interaction of mesenchymal stromal cells (MSCs) with natural killer (NK) cells is traditionally thought of as a static inhibitory model, whereby resting MSCs inhibit NK cell effector function. Here, we use a dynamic *in vitro* system of poly(I:C) stimulation to model the interaction of NK cells and tissue-resident MSCs in the context of infection or tissue injury. The experiments suggest a time-dependent system of regulation and feedback, where, at early time points, activated MSCs secrete type I interferon to enhance NK cell effector function, while at later time points TGF- β and IL-6 limit NK cell effector function and terminate inflammatory responses by induction of a regulatory senescent-like NK cell phenotype. Importantly, feedback of these regulatory NK cells to MSCs promotes survival, proliferation, and pro-angiogenic properties. Our data provide additional insight into the interaction of stromal cells and innate immune cells and suggest a model of time-dependent MSC polarization and licensing.

INTRODUCTION

Providing effective immunity against pathogens and maintaining tissue homeostasis involves a complex coordinated interaction between the immune system and host tissue. Tissue-resident mesenchymal stromal cells (MSCs) form a primary judgment mechanism in this process as they interpret pathogen and cytokine stimuli, leading to induction of inflammation or tissue repair (Bernardo and Fibbe, 2013; Delarosa et al., 2012). MSCs are multipotent fibroblast-like cells that are renowned as potent mediators of anti-inflammatory processes (Prockop and Oh, 2012). Concepts such as “cell empowerment” and “cell replacement” describe how MSCs coordinate the immune system and simultaneously provide a pool of undifferentiated cells for forming new tissue (Wang et al., 2014). The regulatory properties of MSCs combined with easy isolation and expansion have led to their use as a prominent candidate for cellular therapy, and understanding their immunobiology is therefore critical in optimizing their use.

MSCs are equipped with Toll-like receptors (TLRs), which are essential in pathogen recognition as they sense conserved structural motifs in pathogens (pathogen-associated molecular patterns [PAMPs]) (Delarosa et al., 2012; Jakob et al., 2010). Increasing evidence suggests that triggering of TLRs on MSCs modulates both their differentiation potential and immunoregulatory properties (Pevsner-Fischer et al., 2007; Stagg, 2007; Hwang et al., 2014). Using the viral PAMP poly(I:C), which mimics double-stranded viral RNA, we previously demonstrated that TLR3-stimulated MSCs were pro-inflammatory in nature, producing

interferon- α/β (IFN- α/β), interleukin-6 (IL-6), and IL-8 (Dumitru et al., 2014). Here we explored the immunological consequences of this stimulation and asked how poly(I:C)-stimulated MSC could regulate key players of innate antiviral immunity such as natural killer (NK) cells.

NK cells are innate immune cells endowed with the capability to kill virally infected, stressed, and cancerous cells. They are also an important source of IFN- γ , which drives pro-inflammatory Th1 responses (Vivier et al., 2008). On the other hand, NK cells can also exert regulatory functions. For example, during pregnancy CD56^{bright} and senescent NK cells interact with stroma in the decidua to induce angiogenesis and trophoblast invasion (Hanna et al., 2006; Arck and Hecher, 2013; Rajagopalan and Long, 2012).

Only few studies have investigated the interaction of NK cells with MSCs. In pioneering work, the Moretta group has shown that resting unstimulated MSCs are capable of inhibiting NK cell proliferation, cytokine release, and cytotoxicity, via prostaglandin E₂ and indoleamine dioxygenase (Spaggiari et al., 2006, 2008). More recently, evidence is emerging to show that in the proper context MSCs may also support NK cell function (Thomas et al., 2014).

In contrast to most previous work investigating unidirectional MSC-NK cell interaction (i.e., MSC regulation of NK cells), we envisage that, over time, in an inflammatory setting a bidirectional interaction between MSCs and NK cells is likely to exist. Therefore we investigated how TLR-activated MSCs regulate NK cells and then examined the NK cell feedback onto MSCs.



RESULTS

Biphasic, Time-Dependent Response of Poly(I:C)-Stimulated MSCs

Previous studies focusing on MSC regulation of NK cell function demonstrate that resting MSCs are capable of inhibiting NK cell effector function. In contrast to this static model, we stimulated MSCs with poly(I:C), which, over time, led to a distinct biphasic MSC response (Figures 1A–1C). In an early inflammatory phase, poly(I:C)-activated MSCs rapidly released IFN- α/β , IL-6, and IL-8 within 4–8 hr. Thereafter, from 8 hr to 24 hr, type I IFN levels decreased while IL-6 and IL-8 levels continued to increase and, additionally, the supernatant (SN) became rich in IFN- γ -inducible protein 10 (IP-10), macrophage migration inhibitory factor (MIF), and transforming growth factor β (TGF- β) over this period. Interestingly, IL-6, IL-8, and IP-10 were induced by poly(I:C) whereas MIF and TGF- β were not (Figure 1A). Comparing the ratio of antiviral type I IFN with the regulatory factors (IL-6, IL-8, MIF, and TGF- β) at early time points (4 hr; P4h) and later time points (24 hr; P24h) in SN of poly(I:C)-stimulated MSC revealed a clear shift toward regulatory factors over time (Figures 1B and 1C).

The Biphasic Response of MSCs Differentially Affects NK Cell Phenotype and Function

Next, we analyzed the effects of early type I IFN-enriched SN (P4h) and late “regulatory” SN (P24h) on the expression of activation markers and chemokine receptors on purified NK cells during overnight (18 hr) incubation. Human NK cells consist of two major subsets, an immature cytokine producing CD56^{bright}CD16⁻ subset and a more abundant mature cytotoxic CD56^{dim}CD16⁺ subset. No significant changes were induced by the SN of unstimulated and stimulated MSCs in CD56^{bright} NK cells during 18 hr of culture. In contrast, in CD56^{dim} NK cells the 4-hr SN of poly(I:C)-stimulated MSCs (P4h) induced a significant upregulation of CD69. Of note, a very substantial upregulation of CXCR4, which is associated with regulatory decidual NK cell function (Arck and Hecher, 2013; Cerdeira et al., 2013), was observed in CD56^{dim} NK cells exposed to the 24-hr SN of poly(I:C)-stimulated MSCs (P24h) (Figure 1D).

On examining NK cell function, the P4h SN, but not SN of unstimulated MSCs or MSCs stimulated for 24 hr, strongly upregulated cytotoxicity (Figure 2A) and degranulation (Figure 2B) of purified NK cells against K562 targets. As NK cell cytotoxicity is dictated by the net signal of activating and inhibitory receptors, we next analyzed the expression repertoire of NK cell receptors, but no conspicuous receptor change was found (Figure 2C). However, when NK cells were incubated with K562 a significant cor-

relation between the expression levels of CD69 activation marker expression and CD107a degranulation marker was observed (Figure 2D). Regarding NK cytokine production, stimulation with P4h in the presence of IL-12 and IL-18 increased IFN- γ production over controls, while P24h had the opposite effect (Figure 2E). To test the functional relevance of the IFN- α/β present in P4h SN, inhibitory antibodies to type I IFN were added during NK cell stimulation. Both cytotoxicity and IFN- γ production were reduced to background levels by this treatment (Figures 2F and 2G). These data identify type I IFN as a major inducer of NK cell effector function in our system.

In sum, our experiments revealed that early and late SN of poly(I:C)-stimulated, but not unstimulated MSCs, differentially affect function and expression of functional surface molecules on human NK cells. These data also suggest that, upon appropriate stimulation, MSCs may serve as accessory cells by secreting IFN- α/β to upregulate classical NK cell effector functions.

The MSC Regulatory Response Functionally Impairs NK Cells and Induces Apoptosis

As the P24h SN was shown to induce NK expression of CXCR4, a receptor that is closely associated with NK cell development, senescence, and angiogenesis (Cerdeira et al., 2013; Rajagopalan and Long, 2012; Arck and Hecher, 2013), we next evaluated the capacity of the P24h SN to modulate NK cell differentiation. NK cells were therefore exposed to P24h SN for up to 5 days, and CXCR4 expression, phenotype, function, and viability were assessed.

We found that CXCR4 was significantly upregulated by P24h SN within 1 day, declined thereafter, but remained above expression levels seen in all other conditions (Figure 3A). In addition, an increased percentage of the CD56^{dim}CD16⁻ NK cell subset was also observed in the presence of P24h SN at day 5 (Figure 3B). Increase of CD56^{dim}CD16⁻ NK cells strongly correlated with a decrease in CD56^{dim}CD16⁺ NK cells rather than CD56^{bright} NK cells (Figure 3C). Thus, these data are consistent with a scenario in which the P24h SN acts on the CD56^{dim}CD16⁺ cytotoxic NK cell subset, inducing the loss of CD16 to generate a CD56^{dim}CD16⁻ NK cell subset.

This change in NK cell phenotype was also accompanied by a change in NK cell function. Comparing NK cells differentiated in unstimulated (M24h) SN versus P24h SN for 3 days reveals a downregulation of IFN- γ , perforin (Figure 3D), degranulation, and cytotoxicity (Figure 3E) in NK cells. Based on these findings we next tested whether the SN of stimulated MSCs may induce senescence in NK cells. Interestingly, after 3 days of P24h SN treatment, NK cells began to exhibit features of senescence by upregulating senescence-associated genes *uPAR* and *SOCS1* (Figure 3F) (Rajagopalan and Long, 2012). IL-6 and IL-8 are

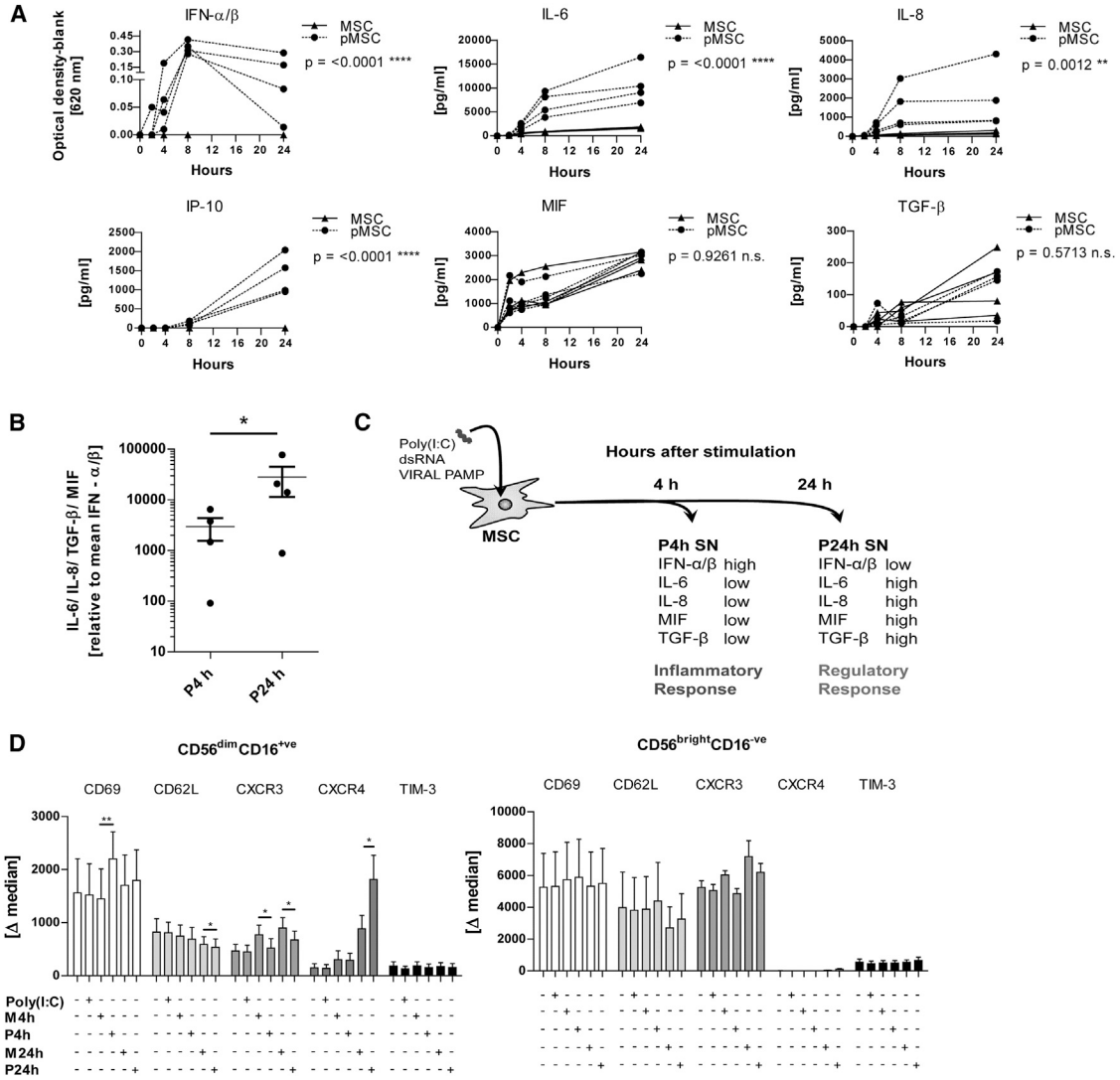


Figure 1. Poly(I:C)-Stimulated MSCs Show a Time-Dependent Response that Modulates NK Cell Phenotype

(A) MSCs were stimulated with poly(I:C) or left resting in medium, and SN was collected at 2, 4, 8, and 24 hr. Cytokines were measured by ELISA and bioassay (n = 4 MSC donors). MSC, unstimulated MSCs; pMSC, poly (I:C)-stimulated MSCs. The statistical analysis and p value shown refers to the comparison of the unstimulated and poly(I:C)-stimulated MSC groups.

(B) The mean concentration of regulatory factors IL-6, IL-8, TGF-β, and MIF relative to the mean concentration of IFN-α/β in poly(I:C)-stimulated MSC SN at time points 4 hr (P4h) and 24 hr (P24h).

(C) Diagram showing the principle of NK cell stimulation using poly(I:C)-stimulated MSC SN (pMSC).

(D) NK cells were incubated overnight (18 hr) with SN from poly(I:C)-stimulated MSCs (P4h and P24h), unstimulated MSC SN (M4h and M24h), poly(I:C) alone, and medium. The expression of NK cell surface markers was measured for both CD56^{bright}CD16⁻ and CD56^{dim}CD16⁺ NK subsets. The delta median (marker expression minus the isotype) is shown (n = 3–5 donors).

Two-way ANOVA and paired t test were used to test statistical significance (p < 0.05 considered as significant). Data are depicted as line graphs (each individual donor) (A), vertical scatter plot (mean ± SE) (B), or bar graphs (mean ± SE) (D). *p < 0.05, **p < 0.01, ****p < 0.0001; n.s., not significant.

key cytokines of the so-called senescence-associated secretory phenotype (SASP) (Perez-Mancera et al., 2014). The ability of NK cells to produce IL-6 along with IL-8 was therefore tested by incubating NK cells with P24h SN in conjunction with IL-12 and IL-18 for 3 days. It is important

to state that unlike MSCs, which will produce IL-6 and IL-8 after poly(I:C) stimulation, NK cells require the presence of IL-12 and IL-18 to induce cytokine production. NK cell production of both SASP factors, IL-6 and IL-8, was greatly increased in P24h SN compared with control M24h SN

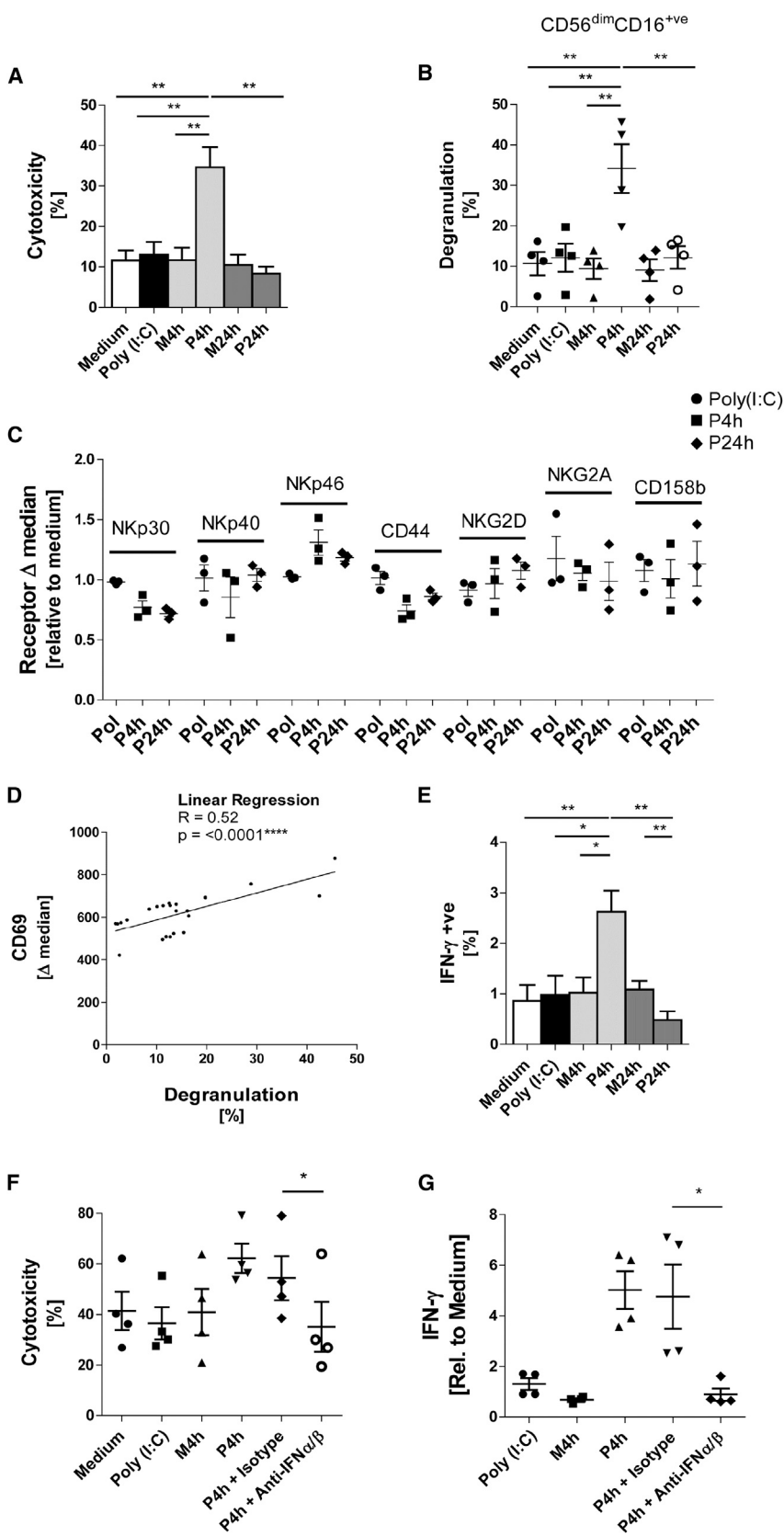


Figure 2. NK Cell Effector Functions Are Promoted by the Inflammatory Early Response from Poly(I:C)-Stimulated MSCs

(A) NK cells were incubated overnight with P4h, P24h, M4h, and M24h SN, with poly(I:C) alone and medium. The cytotoxicity of the NK cells was tested against K562 targets at a 1:2 effector/target (E/T) ratio for 3 hr (n = 5 donors).

(B) NK cells were incubated overnight with the indicated conditioned medium. Degranulation of CD56^{dim}CD16⁺ NK cells against K562 was assessed using the CD107a assay (n = 4).

(C) NK cells were incubated overnight with conditioned medium and expression of surface receptors was measured by flow cytometry. Data are shown as the delta median (marker expression minus the isotype) relative to medium control (n = 3).

(D) NK cells were stimulated overnight with conditioned medium (as in A and B). CD107a assay and flow cytometry for CD69 were performed (n = 4).

(E) NK cells were incubated with conditioned medium in the presence of monensine, IL-12, and IL-18. After 6 hr NK cells were stained for intracellular IFN-γ and the percentage of IFN-γ-positive NK cells was determined (n = 5 donors).

(F) NK cells were incubated overnight with the indicated conditioned medium in the presence of neutralizing antibodies to IFN-α (1 μg/mL) and IFN-β (1 μg/mL) or isotypes as indicated. Degranulation of CD56^{dim}CD16⁺ NK cells against K562 was assessed using the CD107a assay (n = 4).

(G) NK cells were incubated with conditioned medium in the presence of monensine, IL-12, and IL-18; additionally neutralizing IFN-α (1 μg/mL) and IFN-β (1 μg/mL) or isotypes were added where indicated. After 6 hr NK cells were stained for intracellular IFN-γ and the percentage of IFN-γ-positive NK cells was determined (n = 4).

Two-way paired t test and linear regression model was used for statistical analysis, A *p < 0.05 was considered significant and **p < 0.01 or ****p < 0.0001 very significant. Data are depicted as bar graphs (mean ± SE) (A and E), vertical scatter graphs (mean ± SE) (B, C, F, G), and scatter graph (D).

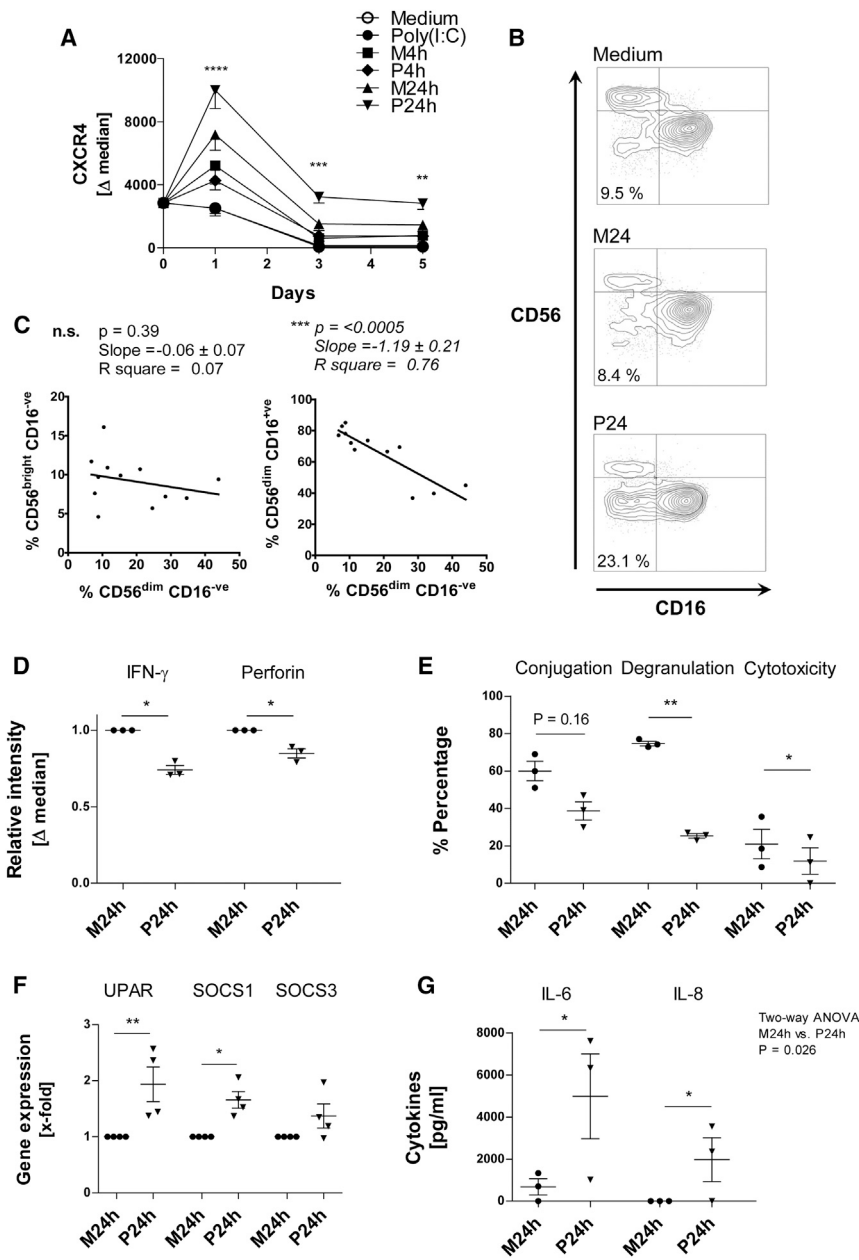


Figure 3. NK Cells Are Functionally Impaired and Undergo Differentiation to a Senescent-like Phenotype, Following Treatment with Regulatory Late-Response SN from Poly(I:C)-Stimulated MSCs

(A) NK cells were incubated for 5 days with poly(I:C)-stimulated MSC SN (P4h and P24h), unstimulated MSC SN (M4h and M24h), poly(I:C) alone, and medium. At days 0, 1, 3, and 5, NK cells were collected and stained for CXCR4; data are shown as the delta median (marker expression minus the isotype). The asterisks refer to the significance between the P24h sample and the poly(I:C) sample at the given time point ($n = 3$ donors).

(B) NK cells were incubated for 5 days in conditioned medium, and were then stained for CD56 and CD16 (scatter plots show staining and NK subsets, 1 representative experiment of 4).

(C) Plots of the percentage of $CD56^{dim}CD16^{+}$ and $CD56^{bright}CD16^{-}$ against the $CD56^{dim}CD16^{-}$ NK subsets ($n = 4$).

(D) NK cells were treated for 3 days with conditioned medium after which the cells were stimulated with PMA/ionomycin in the presence of monensine for 6 hr. NK cells were then stained for intracellular IFN- γ and perforin. Bar graph shows delta median relative to M24h SN-treated NK cells ($n = 3$).

(E) NK cells were treated for 3 days with conditioned medium and their ability to form conjugates, and degranulate and kill K562 target at a 1:2 E/T ratio was assessed ($n = 3$).

(F) NK cells were treated for 3 days with conditioned medium; cells were then lysed and qPCR performed. *uPAR*, *SOCS1*, and *SOCS3* expression was determined. The bar graph shows gene expression relative to M24h-treated NK cells.

(G) NK cells were treated for 3 days with conditioned medium in the presence of IL-12 (10 ng/mL) and IL-18 (10 ng/mL). The

production of NK cell-derived IL-6 and IL-8 was then measured (note that the MSC SN already contained IL-6/IL-8 produced by MSC, so to ascertain the NK cell-derived cytokine levels, the concentration of cytokines in MSC SN without NK cells was subtracted from the concentration of cytokines in MSC SN after NK cell incubation, thus the production of NK cell IL-6 and IL8 could be calculated) ($n = 3$). Data analysis was performed using two-way ANOVA with an additional Bonferroni post test, paired two-tailed t test, and linear regression model. * $p < 0.05$ was considered significant and ** $p < 0.01$, *** $p < 0.001$, or **** $p < 0.0001$ very significant; n.s., not significant. Data are depicted as vertical scatter graphs (mean \pm SE) (D, E, F, and G), line graph (mean \pm SE) (A), and scatter plots (B and C).

(Figure 3G). Moreover, P24h SN-treated NK cells showed increased expression of annexin V/7AAD, reduced size, and increased granularity, and started to form apoptotic bodies (Figures 4A, 4C, and 4D). Expression of p16 in NK cells was also upregulated following P24 SN treatment (Fig-

ure 4B). Mammalian target of rapamycin (mTOR) is a central pathway in NK cell development and differentiation (Marcais et al., 2014). As expected, IL-15 induced the phosphorylation of mTOR in NK cells (Figure 4E). However, P24h MSC SN did not influence this phosphorylation,

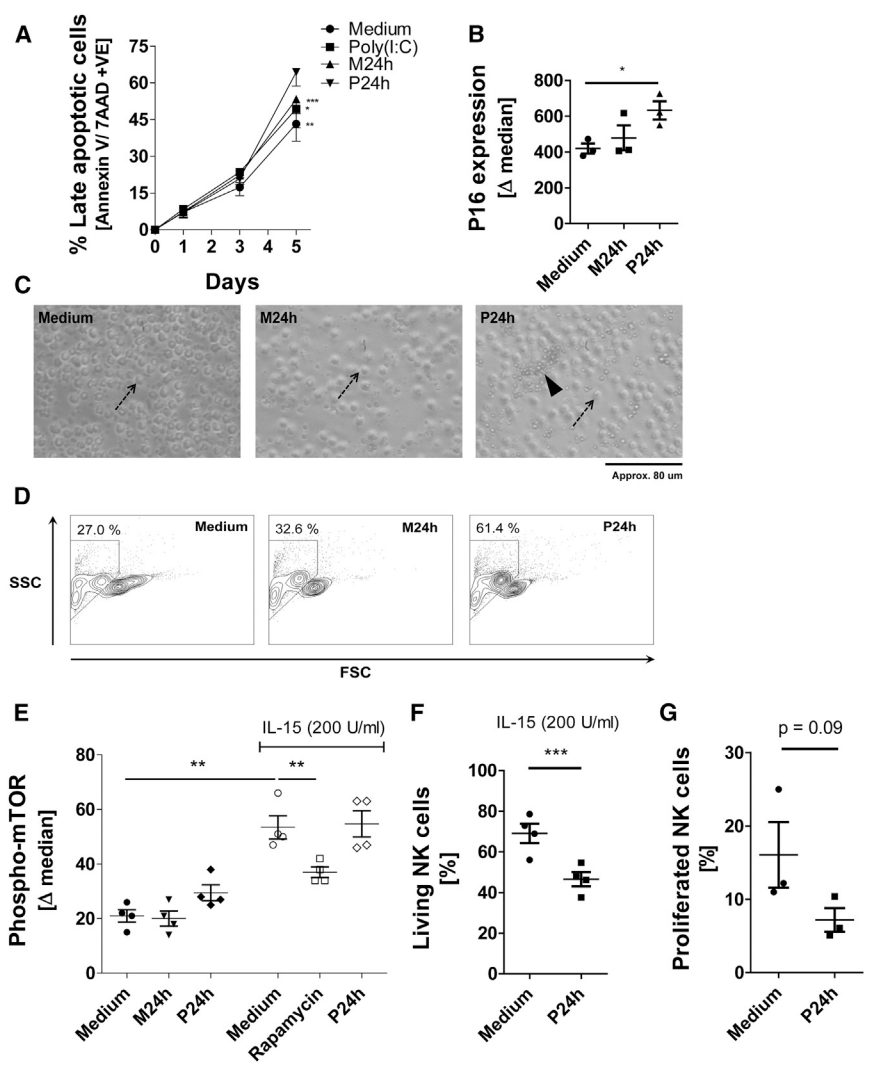


Figure 4. Increased NK Cell Death Following Prolonged Treatment with Regulatory Late-Response SN from Poly(I:C)-Stimulated MSCs

(A) NK cells were incubated for 5 days with (P24h), (M24h), poly(I:C) alone, and medium. At days 1, 3, and 5 NK cells were collected and stained for annexin V and 7AAD, and the percentage of NK cells showing late-stage apoptosis (i.e., annexin V and 7AAD double-positive) evaluated (n = 5 donors).

(B) NK cells were treated for 1 day with conditioned medium and expression of CDKN2A/p16INK4a (P16) was determined by flow cytometry (n = 3).

(C) NK cells were incubated for 9 days in the presence of conditioned medium, and bright-field micrographs were taken at a magnification of $\times 200$; the arrows indicate an intact cell and the arrowhead indicates apoptotic bodies (1 representative experiment of 4 NK donors).

(D) NK cells were incubated for 9 days in the presence of conditioned medium and were then analyzed using flow cytometry for granularity (SSC) and size (FSC) (1 representative experiment of 4 NK donors).

(E) NK cells were incubated with conditioned medium and also in the presence of activating IL-15 with medium, rapamycin (mTOR inhibitor), and P24h SN. After 2 days the cells were stained for phosphorylated mTOR by flow cytometry (n = 4).

(F) NK cells were incubated in conditioned medium for 9 days in the presence of activating IL-15. Percentage of living cells was determined by annexin V and staining (n = 4).

(G) NK cells were labeled with CFSE and then incubated for 5 days with conditioned medium in the presence of IL-15 (200 U/mL) and IL-18 (10 ng/mL). Proliferated cells were quantified as CFSE low cells (n = 3). Data analysis was performed using a paired two-tailed t test and linear regression model. a *p < 0.05 was considered significant and **p < 0.01 or ***p < 0.005 very significant. Data are depicted as vertical scatter graphs (mean \pm SE) (B, E, F, and G), line graph (mean \pm SE) (A), and scatter plot (D).

suggesting that this pathway is not influenced by poly(I:C)-stimulated MSCs. In contrast, the viability and proliferation of NK cells in the presence of cytokines was again considerably reduced in the presence of P24h MSC SN (Figures 4F and 4G).

In conjunction, these data indicate that key hallmarks associated with senescence and cellular death could be induced in NK cells by the P24h SN.

Bone Marrow-Derived MSCs Modulate NK Cells in Similar Manner to Nasal Mucosa-Derived MSCs

In the next series of experiments we tested whether the modulation of NK cells by poly(I:C)-stimulated nasal

mucosal MSCs was shared by bone marrow-derived MSCs (bmMSCs), an MSC type often used in cellular therapy. As shown in Figure S1A CD56^{dim}CD16⁺ NK cells highly express the activation marker CD69 following P4h SN incubation (for corresponding nasal MSC data, see Figure 1D). Both P4h and P24h SN have the capacity to increase NK cell degranulation compared with control (Figure S1B), suggesting that P24h SN of bmMSCs exceeds mucosal MSC stimulatory capacity. Importantly, and similar to nasal MSCs, the bmMSC P24h SN induced senescent-like processes in NK cells (Figures S1C, S1D, and S1E). Also, p16 was upregulated following P24h SN (corresponding nasal MSC data, Figure 4B); and NK cells began to express



CXCR4 along with the lineage subshift of CD56^{dim}CD16⁺ to CD16⁻ (corresponding nasal MSC data, [Figures 3A and 3B](#)). These data indicate that key features of NK cell modulation are shared between MSCs obtained from bone marrow and nasal mucosa. The experiments also reinforce earlier findings ([Brandau et al., 2014](#)), which likewise suggest that the response to TLR stimulation and innate immune interaction is shared between bmMSCs and MSCs from peripheral tissues.

MSC-Derived TGF- β and IL-6 Induce NK Cell CXCR4 Expression and Cell Death

Data thus far show that prolonged stimulation of MSCs with poly(I:C) generated a secretome (P24h SN), which up-regulated CXCR4 expression on NK cells together with loss of NK cell effector function and induction of a senescence-like phenotype. TGF- β and IL-6 in P24h SN were considered possible factors which mediate this mechanism of NK regulation. Both cytokines have been implicated in inducing CXCR4 as well as differentiating lymphocytes and driving senescence/apoptosis ([Arck and Hecher, 2013](#); [Cerqueira et al., 2013](#); [Zhang et al., 2005](#)). Furthermore, these cytokines are found in abundance in the P24h SN although it is only the IL-6 that is poly(I:C) dependent.

TGF- β and IL-6 were measured in various P24h SN derived from various donors, and the level of NK cell CXCR4 induction was analyzed for each SN. Low and high TGF- β /IL-6 ratios were related to CXCR4 expression. As shown in [Figure 5A](#), a high TGF- β /IL-6 ratio in the SN of P24h-stimulated MSCs resulted in higher expression of CXCR4 on NK cells exposed to this SN. Using recombinant TGF- β and IL-6 we found that TGF- β induced NK cell CXCR4 as a single agent, while IL-6 was able to enhance the effect of TGF- β when both cytokines were combined ([Figure 5B](#)). Treating P24h SN with neutralizing antibodies for TGF- β and IL-6 confirmed that these factors in the SN are responsible for NK cell CXCR4 expression ([Figure 5C](#)). We next performed a dose-response curve of TGF- β -induced NK cell CXCR4 in the presence and absence of IL-6 ([Figure 5D](#)). Interestingly, IL-6 antagonized CXCR4 induction at low TGF- β concentrations, but enhanced CXCR4 induction at high concentrations of TGF- β ([Figure 5D](#)). These data reinforce the previously described pleiotropic nature of IL-6 ([Fernando et al., 2014](#); [Scheller et al., 2011](#)) and suggest that the poly(I:C)-dependent factor IL-6 becomes a modulator of the constitutively produced TGF- β , and will inhibit or amplify the effects of TGF- β according to its concentration. Similar to P24h SN, recombinant TGF- β and IL-6 also induced apoptosis in NK cells, reduced CD16 expression, and impaired cytotoxicity against K562 targets ([Figures 5E, 5F, and 5G](#)). These data provide evidence that TGF- β and IL-6 contained in the P24h SN are involved in the regulation of

NK cell function and differentiation observed in our system.

Senescent-like NK Cells Favor MSC Functions, which Are Associated with Tissue Regeneration

SASP released by decidual NK cells has been reported to stimulate angiogenesis ([Rajagopalan and Long, 2012](#)), which requires the coordinated response of stromal and endothelial cells. In the final part of our study we wanted to model the bidirectional interaction of MSCs and NK cell and so tested the feedback effects of our senescent-like NK cells on MSCs. To this end, NK cells were treated for 4 days with P24h SN (= senescent-like NK) or M24h SN (= NK) to induce specific NK cell types.

When using MSCs as target cells, the survival of MSCs from NK cytotoxicity was increased with senescent-like NK cell effectors, consistent with their impaired cytotoxic function ([Figure 6A](#)). Of particular note, senescent-like NK cells still seem to undergo an intense type of interaction with MSCs yet show reduced degranulation ([Figure 6B](#)). Furthermore, NK/MSK cell-cell interaction did not affect the production of TGF- β by MSCs, but did trigger the release of IL-6, which may result in further enhancement of the regulatory NK cell response ([Figures 6C and 6D](#)).

To evaluate the effect of NK cell SASP on MSCs, NK cells were subjected to control medium, M24h, or P24h SN for 2 days, and then washed and resuspended in normal medium for 3 days to allow the NK cells to release their SASP. This NK cell SASP was next incubated with MSCs for 24 hr, and gene expression, invasion, and proliferation of MSCs were then examined ([Figures 6E, 6G, and 6H](#)). The senescent-like NK cells induced a highly significant increase in *VEGF* gene expression by MSCs ([Figure 6E](#)). The SN derived from these MSCs was also able to increase tube formation in human microvascular endothelial cells ([Figure 6F](#)). Finally, senescent-like NK cells significantly increased the proliferation of MSCs but not the invasive capacity when compared with medium control ([Figures 6G and 6H](#)).

In sum, these data suggest that senescent-like NK cells, which are induced by poly(I:C)-stimulated MSCs, exert feedback on MSCs. During this feedback, senescent-like NK cells favor tissue-regenerative functions of MSCs over MSC killing.

MSC and NK Cell Interaction: A Stable System of Inflammation and Repair

[Figure 7](#) illustrates the bidirectional and time-dependent interaction of MSCs and NK cells in the context of poly(I:C) stimulation as shown in this article. [Figure 7](#) also shows how MSC-NK interaction may potentially contribute to antipathogen immunity, inflammation, and tissue repair.

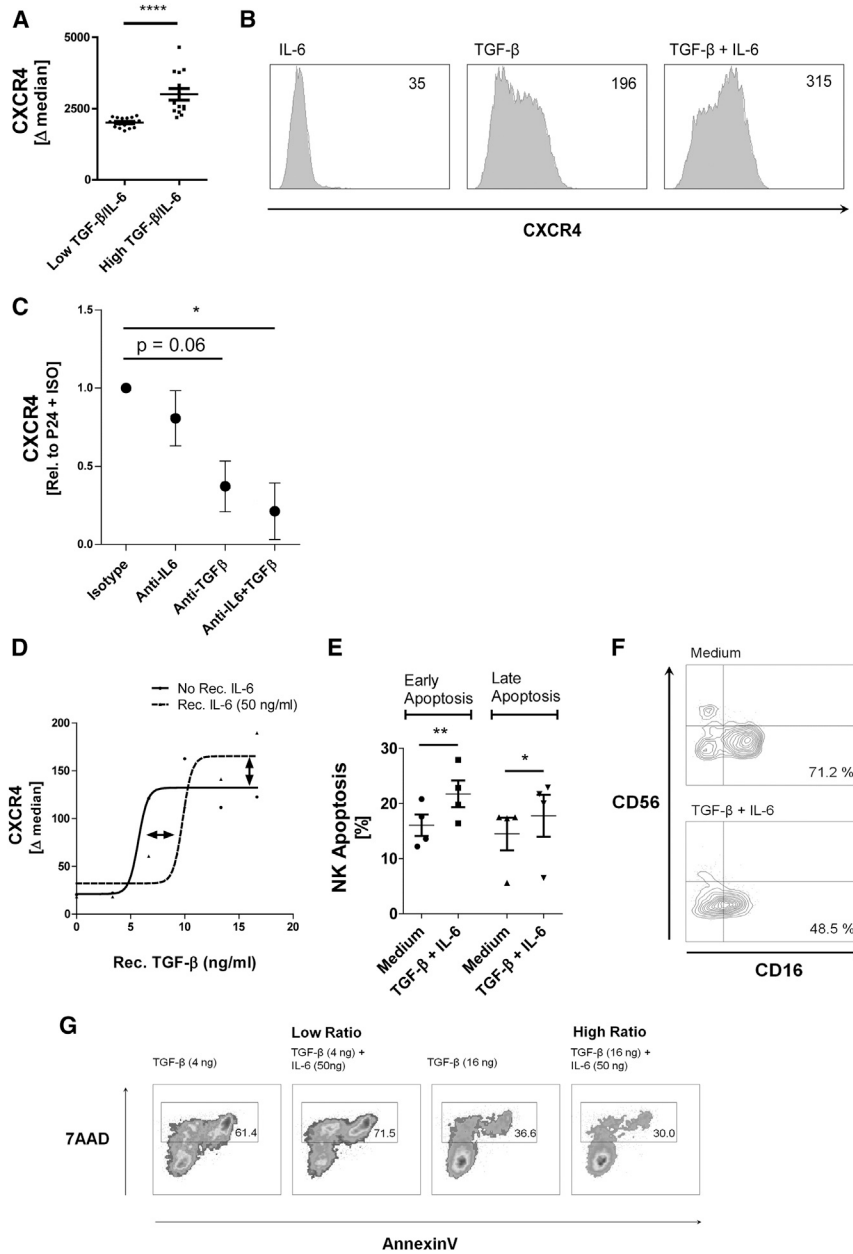


Figure 5. TGF- β and IL-6 Limit NK Cell Cytotoxicity and Induce CXCR4 Expression as well as NK Cell Apoptosis

(A) NK cells were incubated for 1 day with 16 independently generated P24h SN. Ratio of IL-6 and TGF- β in the SN was calculated and plotted against the capacity of the SN to induce NK CXCR4. The data allowed a non-linear regression sigmoidal dose-response curve to be fitted, which predicted an EC₅₀ of 12.5. The predicted EC₅₀ was used as a cutoff to divide low IL-6/TGF- β ratio SN (below EC₅₀) and high IL-6/TGF- β ratio SN. The CXCR4 expression of the NK cells was sorted according to this criterion and a vertical scatter plot generated (the IL-6 and TGF- β high/low ratio relationship to CXCR4 can also be seen in the dose-response curves of D).

(B) Histograms of NK CXCR4 following overnight incubation with recombinant IL-6 (50 ng/mL) alone and TGF- β (16 ng/mL) alone and in combination (1 representative experiment of 4 NK donors).

(C) NK cells were cultured in P24h SN for 2 days in the presence of inhibitory antibodies to IL-6 (1 μ g/mL) and TGF- β (1 μ g/mL) or isotypes as indicated. Expression of CXCR4 on NK was measured (n = 3 donors).

(D) Recombinant IL-6 and TGF- β were incubated with NK cells for 2 days. The expression of CXCR4 was then measured and a non-linear regression sigmoidal dose-response curve was plotted (n = 2).

(E) NK cells were treated for 2 days with a combination of recombinant IL-6 (50 ng/mL) and TGF- β (16 ng/mL), the cells were then stained for annexin V-positive NK cells (representing early apoptosis) and annexin V-positive 7AAD-positive NK cells (representing late apoptosis) (n = 4).

(F) NK cells were treated for 2 days with a combination of recombinant IL-6 (50 ng/mL) and TGF- β (16 ng/mL) and then stained for CD56 and CD16. Percentage of the CD56^{dim}CD16⁺ subset from the entire NK cell population is shown (1 representative experiment of 4 NK donors).

(G) NK cells were treated for 2 days with TGF- β and IL-6 at low and high concentration ratios. Cytotoxicity of the NK cells was then tested against K562 targets. Gate indicates percentage of killed target cells (1 representative experiment of 2 NK donors). Data analysis was performed using a paired two-tailed t test and non-linear regression dose-response model. *p < 0.05 was considered significant and **p < 0.01 or ****p < 0.0001 very significant. Data are depicted as histograms (y axis is count) (B), line graph (mean \pm SE) (D), vertical scatter plot (mean \pm SE) (A, C, and E), and scatter plots (F and G).

DISCUSSION

Previous reports have focused on the intrinsic anti-inflammatory properties of resting MSCs, and showed inhibitory activity on classical NK cell effector functions such as cyto-

toxicity and IFN- γ production (Chatterjee et al., 2014; Spaggiari et al., 2006, 2008; Pradier et al., 2011). These experiments are likely to explain the interaction of MSCs and NK cells in a steady-state scenario; however, such models do not address the critical interaction between these cell

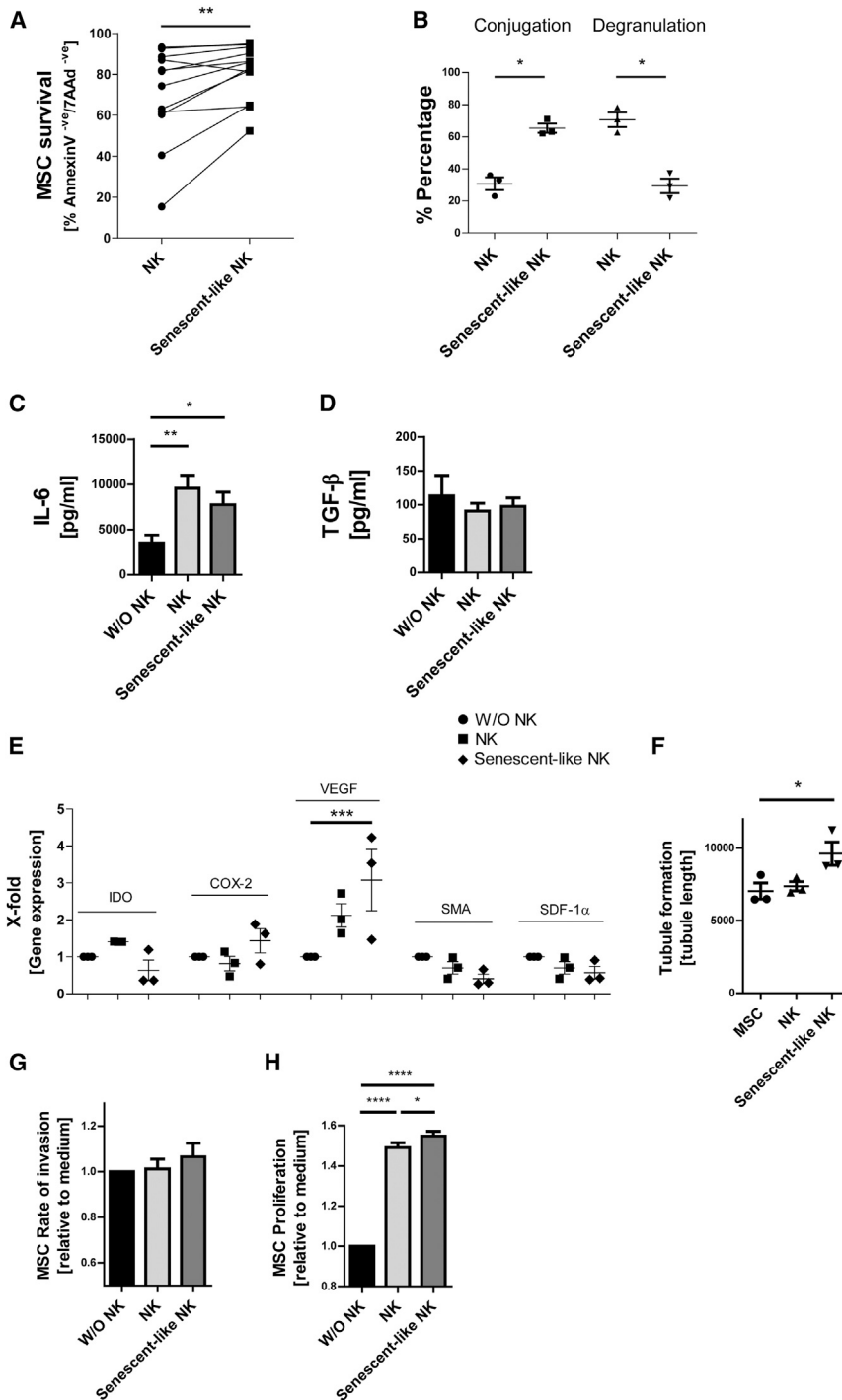


Figure 6. Senescent-like NK Cells Favor MSC Survival and Proliferation

(A) NK cells were incubated for 3 days with poly(I:C)-stimulated MSC SN (P24h) to generate senescent-like NK cells or were incubated with unstimulated MSC SN (M24h) as a control (NK). Killing of MSC by NK cells or senescent-like NK cells was assessed using annexin V/7AAD staining (n = 12). Percentage of double-negative living MSCs is shown.

(B) Senescent-like NK cells or control NK cells (as in A) were labeled with CFSE. Conjugate formation with MSC and CD107a degranulation against MSC targets was assessed. Percentage of NK cells forming conjugates and percentage of CD107a⁺ NK cells was determined (n = 3).

(C and D) Senescent-like NK cells or control NK cells (as in A and B) were incubated for 24 hr with a monolayer of MSCc (at a ratio of 1 NK cell to 5 MSCs). The SN of the co-cultures was then collected and IL-6 (C) or TGF-β (D) concentration measured (n = 4 donors).

(E) Gene expression of MSCs following 24-hr incubation with medium only (without [W/O] NK cells) or SN generated from conditioned NK cells (n = 3).

(F) Pooled SN from senescent-like or control NK cells was generated from three NK cell donors. MSCs were stimulated for 24 hr with medium only (MSC) or SN generated from conditioned NK cells. The MSC-NK-SN was collected and incubated overnight with a human microvascular endothelial cell line. Tubule formation was analyzed and average tube length recorded (n = 3).

(G) An invasion assay was performed using MSCs incubated in the presence of medium only (without NK cells) or SN generated from conditioned NK cells. The rate of invasion was analyzed over 3 days and assessed by measuring the area of uninvaded space (n = 3 MSC donors and 3 NK cell donors).

(H) Equal numbers of MSC were incubated in the presence of medium only (without NK cells) or SN generated from conditioned NK cells for 5 days. MSC proliferation was analyzed by MTT assay (n = 3 MSC donors and 3 NK donors).

Data analysis was performed using a paired two-tailed t test and two-way ANOVA was performed with an additional Bonferroni post test. *p < 0.05 was considered significant and **p < 0.01, ***p < 0.001, or ****p < 0.0001 very significant. Data are depicted as bar graphs (mean ± SE) (C, D, G, and H) and vertical scatter plots (mean ± SE) (A, B, E, and F).

types in the context of infection and inflammation. Therefore, in this study we explored the consequences of MSC-NK crosstalk in the presence of poly(I:C), a model stimulus

for viral infection. We found that primary MSC of the nasal mucosa responded with a biphasic cytokine response to this challenge. Short-term stimulation of MSCs resulted

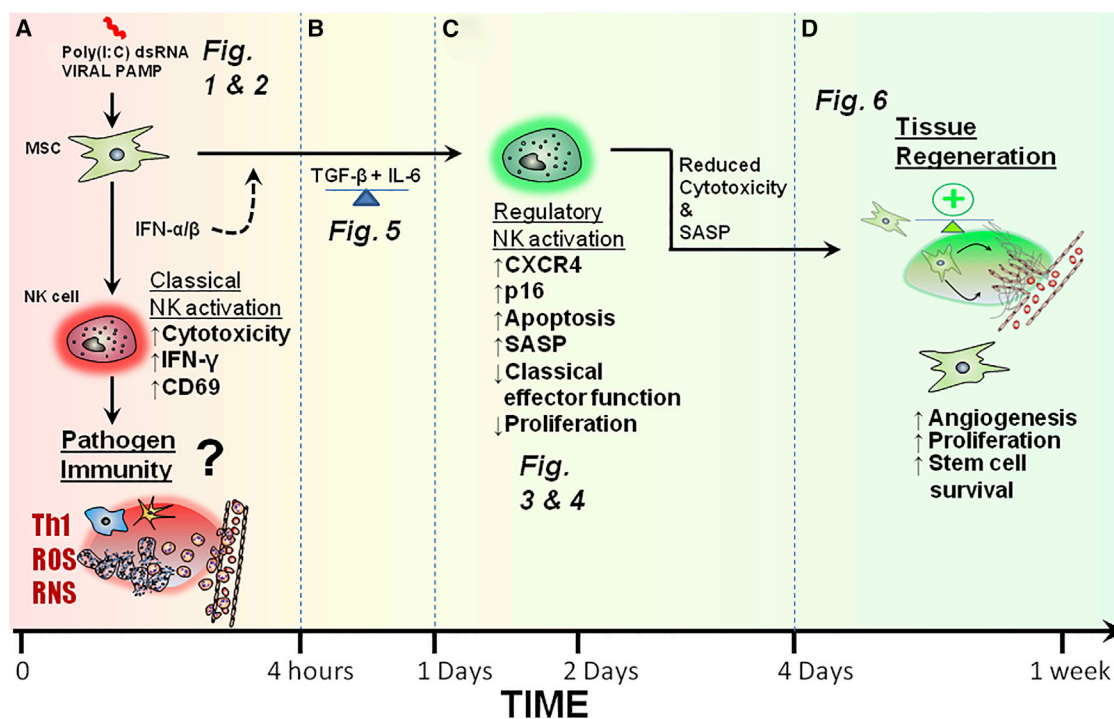


Figure 7. Time-Dependent Polarization of MSCs Differentially Modulates NK Cell Activation and Differentiation

(A) Short-term activation of MSCs by poly(I:C) promotes NK cell activation and pathogen immunity (Figures 1 and 2).

(B) TGF- β and IL-6 produced by activated MSCs limit NK cell effector function and promote NK cell differentiation (Figure 5).

(C) In the context of prolonged MSC stimulation and NK cell interaction, NK cells undergo a senescence-like process and display reduced effector function (Figures 3 and 4).

(D) Senescent-like NK cell feedback on MSCs to promote their survival, proliferation, and pro-angiogenic properties (Figure 6).

in NK cell activation, while longer stimulation of MSCs and prolonged exposure of NK cells to factors secreted by these MSCs led to an NK cell regulatory response. Thus MSC-NK crosstalk in this system mimics the different phases of infection ranging from initial NK cell immunity and inflammation to later termination of NK cell effector function and tissue regeneration (see Figure 7).

An important issue in this study concerns using the MSCs sourced from nasal mucosa. MSCs are found ubiquitously in almost all tissues, but popular sources for cellular therapy include bone marrow, adipose tissue, and Wharton's jelly. In this study MSCs are derived from the nasal mucosa, a highly active immunological site where exposure to pathogens and allergens is a common event. It is sometimes hypothesized that MSCs derived from different source tissues may exhibit differential cell biological properties. Consequently studies were designed to compare the properties and characteristics of MSCs from these different sources. For example, it was suggested that adipose MSCs proliferate faster than bmMSCs and are more suitable for the regeneration of the femoral head following osteonecrosis (Wyles et al., 2015). Placental MSCs show clear phenotypic and transcriptomic differences compared

with bmMSCs (Elahi et al., 2016). Importantly, in Figure S1 we showed here that stimulated bmMSCs regulated NK cells in a manner similar to that of nasal mucosa MSCs. It is certainly possible that cell biological differences still exist between MSCs sourced from the nasal mucosa and bone marrow. However, under the conditions described in this study, their response to poly(I:C) and subsequent immunoregulatory properties are comparable.

In a previous study (Waterman et al., 2010), poly(I:C) stimulation of MSCs was examined in the context of MSC polarization. The authors concluded that stimulating MSCs with poly(I:C) led to an anti-inflammatory type of MSC or MSC2, while lipopolysaccharide stimulation rather induced an inflammatory MSC1. Importantly, in their study Waterman et al. (2010) stimulated MSCs for only 1 hr and then washed the stimuli away. Exposure of 1 hr is probably a rare situation *in vivo* or, as the authors state, rather mimics an MSC that is distant from the site of injury. However, MSCs at an infection site would probably be exposed continuously to TLR agonists for the course of the infection, which may last days as modeled in our study. As poly(I:C) mimics viral double-stranded RNA, our study suggests that MSC polarization in response to viral



stimulation can occur in a time-dependent manner. Rather than being purely anti-inflammatory in nature, the MSC response adapts according to time and course of infection.

Some studies, in contrast to that of [Waterman et al. \(2010\)](#), have shown that TLR3 stimulation of MSCs leads to a pro-inflammatory response ([Cassatella et al., 2011](#); [Kota et al., 2014](#)). However, our data reconcile the dichotomy of how a TLR3-activated MSC can be both pro-inflammatory yet also anti-inflammatory. Upon arriving at an infection site, MSCs may respond in a time-dependent manner, consisting of an initial release of early pro-inflammatory IFN- α/β and then later secreting regulatory factors IL-6 and TGF- β . We also speculate that depending on the phase of wound healing (i.e., inflammatory, proliferative, maturation, and remodeling), MSCs will actively contribute to each phase accordingly and tend to drive the process to completion, leading to restoration of tissue function.

One of the important implications of our study is that MSC stimulation can promote the regenerative function of NK cells. The maternal/fetal interface in the decidua is one of the few reported examples of this. Here NK cells help in constructing the complex capillary network that integrates the blood systems ([Arck and Hecher, 2013](#); [Wu et al., 2005](#)). Trafficking of decidual NK cells is regulated via CXCR4 and these specialized NK cells also display a senescent phenotype that release SASP to induce angiogenesis from stroma, a scenario remarkably similar to the senescent-like feedback of NK cells on MSCs shown in our study ([Rajagopalan and Long, 2012](#); [Rajagopalan, 2014](#); [Hanna et al., 2003](#)). [Cerdeira et al. \(2013\)](#) showed that decidual-like NK cells with angiogenic properties can be induced from peripheral NK cells by treatment with a combination of hypoxia, TGF- β , and demethylating agents. We used a mix of TGF- β and IL-6 to induce regulatory NK cells, which share some features with decidual-like NK cells. Our study supports this hypothesis, and we envisage that the NK-mediated angiogenesis and tissue growth that takes place during trophoblast invasion is also utilized by MSCs in peripheral tissues to induce repair following infection and inflammation. Thus, our study provides insight into the complex interaction of stromal cells and NK cells in the context of infection, and suggests a model of time-dependent MSC polarization.

EXPERIMENTAL PROCEDURES

Human Nasal Mucosa MSC Isolation and Culture

MSCs were derived from the nasal concha of healthy donors who were undergoing reduction of the nasal turbinate at the Department of Otorhinolaryngology, University Hospital, Essen (Germany). The study was approved by the local ethics committee (No. 08-3710). Isolation of nasal mucosa MSCs was performed as

previously described ([Jakob et al., 2010](#)). In brief, tissue samples were minced and treated with collagenase 2 (Sigma-Aldrich, Taufkirchen, Germany) and dispase II (Roche Applied Science, Wiesbaden, Germany). The digested tissue was then strained through a 100- μ m CellTrics (Sysmex Partec, Görlitz, Germany), and seeded in a T75 flask with RPMI 1640/DMEM (high glucose) (50%/50% [v/v], both Thermo Fisher Scientific, Karlsruhe, Germany) culture medium supplemented with 10% fetal calf serum (Biochrom, Berlin, Germany) and 1% penicillin/streptomycin (Thermo Fisher Scientific); all cultures were mycoplasma free. MSCs adhered to the phenotype proposed by the International Society of Cellular Therapy (CD29⁺, CD34⁻, CD45⁻, CD90⁺, CD105⁺) were negative for NG2, presented a fibroblast-like morphology, and were strongly plastic adherent. The MSCs were multipotent and capable of differentiating into mesodermal lineages including osteo-, chondro-, and adipogenic lineages ([Jakob et al., 2010](#)). They were also immunosuppressive as shown by inhibition of T cell proliferation. MSCs were used in experiments between passages 3 and 7.

Human NK Cell Isolation and Culture

NK cells were derived from peripheral blood or buffy coat from healthy donors after written informed consent using guidelines approved by the Ethics Committee of the University Hospital of Essen. NK cells were isolated from peripheral blood mononuclear cells after density-gradient centrifugation via negative selection using NK Isolation Kit II (Miltenyi, Bergisch Gladbach, Germany) according to the manufacturer's instructions. NK cells were cultured in RPMI 1640/DMEM (high glucose; 50%/50% [v/v]) medium supplemented as described above. A subactivating concentration of 5 U/mL IL-15 (Immunotools, Friesoythe, Germany) was always added into NK medium to maintain NK cell viability.

MSC Poly(I:C) Stimulation

For MSC stimulation with poly(I:C) (Sigma-Aldrich), MSCs were seeded overnight in wells of a 24-well plate at 2.5×10^5 per well with 500 μ L of medium. The next day the compact monolayer of MSCs was washed with PBS, and 500 μ L of medium with poly(I:C) (1 μ mol) was added for 4 hr to produce P4h SN or 24 hr for P24h, at which time the SN was collected. As a control, unstimulated MSC SN was also generated in parallel using the same conditions but without poly(I:C), hence M4h and M24h SN. For NK cell experiments using nasal MSC SN, at least three MSC donors were used to produce a pooled SN, and in total 16 different MSC donors were used throughout experiments. For bone marrow-derived SN at least two donors were used, and in total six different MSCs were used throughout experiments.

ELISA

IL-6, IL-8, and TGF- β concentrations in SN were measured using a DuoSet ELISA (R&D Systems, Wiesbaden, Germany) according to the manufacturer's instructions. Absorbance at 450 nm was measured using Synergy 2 Multi-Detections Reader (Biotek, Bad Friedrichshall, Germany).

Quanti-Blue IFN- α/β Bioassay

The concentration of IFN- α/β was measured using the Hek Blue Quanti-Blue bioassay (Invivogen, Toulouse, France) according to



the manufacturer's instructions; all cultures were mycoplasma free. Absorbance at 630 nm was measured using Synergy 2 Multi-Detections Reader (BioTek).

Flow-Cytometric Analysis

All primary antibodies were targeted against human antigens. The antibodies used for analysis included CD16 (clone 3G8, PE-Cy7), CD107a (clone H4A3, fluorescein isothiocyanate [FITC]), IFN- γ (clone B27, APC), CD44 (clone 515, PE, all BD Biosciences), CD56 (clone HCD56, Brilliant Violet 510), CD62-L (clone DREG-56, PerCP/Cy5.5), CXCR4 (clone 12G5, PE), CXCR3 (clone G025H7, APC), neutralizing IL-6 (clone MQ2-13A5), neutralizing IFN- α (clone MMHA6, all Tebu-Bio, Le Perray-en-Yvelines, France), neutralizing IFN- β (PeproTech, Hamburg, Germany), Perforin (clone dG9, FITC, Biolegend, Fell, Germany), TIM-3 (clone F38-2E2, PerCP-eFluor710, eBioscience, Frankfurt, Germany), Nkp30 (clone Z25, RPE), Nkp40 (clone Z231, RPE), Nkp46 (clone BAB281, RPE), NKG2A (clone Z199), CD158b (all Beckman Coulter, Krefeld, Germany), NKG2D (clone 149810, RPE), neutralizing TGF- β 1,2,3 (clone 1D11, both R&D Systems, Wiesbaden, Germany), CDKN2A/p16INK4a (rabbit IgG, Abcam, Cambridge, UK) and phospho-mTOR (rabbit IgG, Cell Signaling, Frankfurt, Germany). As secondary coupled antibodies, goat anti-rabbit Alex488 (Dianova) was used.

Surface/Intracellular Staining

Surface staining employed antibody diluted in azide-phosphate buffer solution and 3% human serum for 30 min at 4°C. For intracellular staining, cells were permeabilized according to the manufacturer's instructions using Cytotfix/Cytoperm (BD Biosciences). Staining was then performed using PermWash (BD Biosciences).

Stimuli and Inhibitors

Stimulants used in experiments included: poly(I:C) (Sigma-Aldrich, Taufkirchen, Germany), ionomycin/PMA (Sigma-Aldrich), IL-12 (PeproTech, Hamburg, Germany), IL-15 (Immunotools), and IL-18 (MBL International, Woburn, USA). Inhibitors used in experiments included the mTOR inhibitor rapamycin (Merck Calbiochem, Darmstadt, Germany).

Conjugation Assays

NK cells were labeled with carboxyfluorescein succinimidyl ester (CFSE) (Thermo Fisher Scientific) according to the manufacturer's instructions. NK cells were incubated with target cell K562 or MSCs (at an effector/target ratio of 1:2 for K562 and 2:1 for MSC) for 1 hr in a 96-well U-bottomed plate with medium. After 1 hr cells were centrifuged and carefully resuspended in PBS. Cells were immediately analyzed using BD FACS Canto II (BD Bioscience) and BD FACSDiva Software 8.0 (BD Bioscience). Percentage of CFSE+NK/target conjugates was assessed by gating on target cells in the forward scatter channel.

Cytotoxicity Assay

NK cells were incubated with targets K562 or MSC (at an effector/target ratio of 1:2 for K562 and 2:1 for MSC) for 3 hr in a 96-well U-bottomed plate in medium; all cultures were mycoplasma free.

Cells were centrifuged and stained with PE Annexin V Apoptosis Detection Kit I (BD Biosciences, Heidelberg, Germany) according to the manufacturer's instructions.

Degranulation Assay

NK cells were incubated with targets K562 or MSCs (at an effector/target ratio of 1:2 for K562 and 2:1 for MSC) for 3 hr in a U-bottomed 96-well plate with medium in the presence of BD GolgiStop (Monensin); all cultures were mycoplasma free. Afterward cells were washed in azide-phosphate buffer solution stained for CD107a FITC and immediately analyzed on BD FACS Canto II.

NK Cell Proliferation Assay

NK cells were labeled with CFSE (Thermo Fisher Scientific) according to the manufacturer's instructions. The NK cells were then incubated with conditioned medium in the presence of 200 U/mL activating IL-15 and 10 ng/mL IL-18 (Immunotools). After 5 days NK cells were measured using a BD FACSCanto II (BD Bioscience) and the percentage of proliferated cells was measured by gating on NK cells with reduced CFSE signal intensity.

qPCR and Primers

Total RNA was purified from MSCs and NK cells using the RNeasy mini kit (Qiagen, Hilden, Germany) according to the manufacturer's instructions and quantified by an average optical density (OD) $OD_{260\text{ nm}}/OD_{280\text{ nm}}$ using a Synergy 2 Multi-Detection-Reader (BioTek). RNA was reverse transcribed using a SuperScript II RNase Reverse Transcriptase kit with Hexamer random primers (both Thermo Fisher Scientific), according to the manufacturer's protocol. Amplification was performed in a My-cycler thermal cycler (Bio-Rad, Munich, Germany). qRT-PCR was performed on diluted cDNA using DyNAmo Capillary SYBR Green qPCR kit (Thermo Fisher Scientific) and Roche LightCycler 2.0 instrument (Roche, Wiesbaden, Germany). Gene expression was quantified using the $2^{-\Delta\Delta C(T)}$ method accordingly (Livak and Schmittgen, 2001). A list of primers and sequences is provided in Table S1.

Senescent-like NK Cell SN

Senescent-like NK cell SN was generated by first treating the NK cells with pMSC24h SN for 2 days to initiate the senescent-like process. NK cells were then washed with PBS and resuspended in normal medium and incubated for a further 4 days before SN was collected and used for experiments.

Angiogenesis and Human Microvascular Cell Line Tubule Formation

Wells of a flat 96-well plate were coated with basement membrane (Cultrex, BME, Biozol, Munich, Germany). Human microvascular endothelial cells were seeded into the wells with conditioned medium and incubated overnight. The next day, pictures were taken using a microscope of tubule formation, and total tubule length was measured using ImageJ.

MSC Invasion Assay

Wells of a flat 96-well plate were coated with basement membrane (Cultrex, BME, Biozol, Munich, Germany) and a plug (Tebu-Bio,



Offenbach, Germany) was applied to cover the center of the well. MSCs were then seeded and incubated overnight around the plug. The next day the plug was removed and conditioned medium added. Images using a microscope were taken over 3 days to assess the extent of MSC invasion by measuring the area of uninvaded or MSC-free space. Images were analyzed using ImageJ.

MTT and MSC Proliferation Assay

MSCs were seeded into wells of a 96-well flat-bottomed plate and allowed to adhere overnight. The next day the MSC medium was removed and replaced with conditioned medium. After 5 days the amount of viable cells was determined by incubation for 3 hr with 250 $\mu\text{g}/\text{mL}$ methylthiazolyldiphenyl-tetrazolium bromide (MTT) (Sigma-Aldrich, Taufkirchen, Germany). Cells were lysed with DMSO and absorbance was measured using a Synergy 2 Multi-Detection Reader (BioTek).

Statistics

All statistical tests were performed using GraphPad Prism5. Mean and SE are shown in bar graphs. At least three independent donors for MSCs and NK cells were used for statistical analysis to ensure reliability of data. Statistical tests used included two-tailed and one-tailed paired t test, linear regression model, non-linear dose-response regression model, and two-way and one-way ANOVA with post Bonferroni testing. A significant p value was set at $*p < 0.05$, and $**p < 0.01$ was considered very significant. In the figure legends the number of independent replicate experiments is indicated by “n.”

SUPPLEMENTAL INFORMATION

Supplemental Information includes Supplemental Experimental Procedures, one figure, and one table and can be found with this article online at <http://dx.doi.org/10.1016/j.stemcr.2017.06.020>.

AUTHOR CONTRIBUTIONS

R.M.P. performed and designed experiments, analyzed data, and wrote the paper; K.H. analyzed data and helped to draft the paper; C.A.D. contributed to the conceptual design and helped to draft the paper; A.H. performed experiments and analyzed data; K.B. performed experiments and analyzed data; S.B.F. provided bone marrow MSC material; A.P. contributed to the conceptual design/interpretation of data as well as drafting of the paper; S.L. provided patient material; S.B. conceived the study, interpreted data, and wrote the paper.

ACKNOWLEDGMENTS

This project was supported by a grant from the Deutsche Forschungsgemeinschaft (DFG, grant no. BR 2278/3-1) to S.B. We are very grateful to all NK cell and MSC donors. We thank Natalia Block for her advice on p16 staining and Petra Altenhoff and Sebastian Vollmer for technical assistance.

Received: August 16, 2016

Revised: June 29, 2017

Accepted: June 29, 2017

Published: August 3, 2017

REFERENCES

- Arck, P.C., and Hecher, K. (2013). Fetomaternal immune cross-talk and its consequences for maternal and offspring's health. *Nat. Med.* *19*, 548–556.
- Bernardo, M.E., and Fibbe, W.E. (2013). Mesenchymal stromal cells: sensors and switchers of inflammation. *Cell Stem Cell* *13*, 392–402.
- Brandau, S., Jakob, M., Bruderek, K., Bootz, F., Giebel, B., Radtke, S., Mauel, K., Jäger, M., Flohé, S.B., and Lang, S. (2014). Mesenchymal stem cells augment the anti-bacterial activity of neutrophil granulocytes. *PLoS One* *9*, e106903.
- Cassatella, M.A., Mosna, F., Micheletti, A., Lisi, V., Tamassia, N., Cont, C., Calzetti, F., Pelletier, M., Pizzolo, G., and Krampera, M. (2011). Toll-like receptor-3-activated human mesenchymal stromal cells significantly prolong the survival and function of neutrophils. *Stem Cells* *29*, 1001–1011.
- Cerdeira, A.S., Rajakumar, A., Royle, C.M., Lo, A., Husain, Z., Thadhani, R.I., Sukhatme, V.P., Karumanchi, S.A., and Kopcow, H.D. (2013). Conversion of peripheral blood NK cells to a decidual NK-like phenotype by a cocktail of defined factors. *J. Immunol.* *190*, 3939–3948.
- Chatterjee, D., Marquardt, N., Tufa, D.M., Hatlapatka, T., Hass, R., Kasper, C., von, K.C., Schmidt, R.E., and Jacobs, R. (2014). Human umbilical cord-derived mesenchymal stem cells utilize activin-a to suppress interferon-gamma production by natural killer cells. *Front. Immunol.* *5*, 662.
- Delarosa, O., Dalemans, W., and Lombardo, E. (2012). Toll-like receptors as modulators of mesenchymal stem cells. *Front. Immunol.* *3*, 182.
- Dumitru, C.A., Hemed, H., Jakob, M., Lang, S., and Brandau, S. (2014). Stimulation of mesenchymal stromal cells (MSCs) via TLR3 reveals a novel mechanism of autocrine priming. *FASEB J.* *28*, 3856–3866.
- Elahi, K.C., Klein, G., Avci-Adali, M., Sievert, K.D., Macneil, S., and Aicher, W.K. (2016). Human mesenchymal stromal cells from different sources diverge in their expression of cell surface proteins and display distinct differentiation patterns. *Stem Cells Int.* *2016*, 5646384.
- Fernando, M.R., Reyes, J.L., Iannuzzi, J., Leung, G., and McKay, D.M. (2014). The pro-inflammatory cytokine, interleukin-6, enhances the polarization of alternatively activated macrophages. *PLoS One* *9*, e94188.
- Hanna, J., Wald, O., Goldman-Wohl, D., Prus, D., Markel, G., Gazit, R., Katz, G., Haimov-Kochman, R., Fujii, N., Yagel, S., et al. (2003). CXCL12 expression by invasive trophoblasts induces the specific migration of CD16⁺ human natural killer cells. *Blood* *102*, 1569–1577.
- Hanna, J., Goldman-Wohl, D., Hamani, Y., Avraham, I., Greenfield, C., Natanson-Yaron, S., Prus, D., Cohen-Daniel, L., Arnon, T.I., Manaster, I., et al. (2006). Decidual NK cells regulate key developmental processes at the human fetal-maternal interface. *Nat. Med.* *12*, 1065–1074.
- Hwang, S.H., Cho, H.K., Park, S.H., Lee, W., Lee, H.J., Lee, D.C., Oh, J.H., Park, S.H., Kim, T.G., Sohn, H.J., et al. (2014). Toll like receptor 3 & 4 responses of human turbinate derived mesenchymal stem



- cells: stimulation by double stranded RNA and lipopolysaccharide. *PLoS One* 9, e101558.
- Jakob, M., Hemed, H., Janeschik, S., Bootz, F., Rotter, N., Lang, S., and Brandau, S. (2010). Human nasal mucosa contains tissue-resident immunologically responsive mesenchymal stromal cells. *Stem Cells Dev.* 19, 635–644.
- Kota, D.J., DiCarlo, B., Hetz, R.A., Smith, P., Cox, C.S., Jr., and Olson, S.D. (2014). Differential MSC activation leads to distinct mononuclear leukocyte binding mechanisms. *Sci. Rep.* 4, 4565.
- Livak, K.J., and Schmittgen, T.D. (2001). Analysis of relative gene expression data using real-time quantitative PCR and the 2(-Delta Delta C(T)) method. *Methods* 25, 402–408.
- Marcais, A., Cherfils-Vicini, J., Viant, C., Degouve, S., Viel, S., Fenis, A., Rabilloud, J., Mayol, K., Tavares, A., Bienvenu, J., et al. (2014). The metabolic checkpoint kinase mTOR is essential for IL-15 signaling during the development and activation of NK cells. *Nat. Immunol.* 15, 749–757.
- Perez-Mancera, P.A., Young, A.R., and Narita, M. (2014). Inside and out: the activities of senescence in cancer. *Nat. Rev. Cancer* 14, 547–558.
- Pevsner-Fischer, M., Morad, V., Cohen-Sfady, M., Rouso-Noori, L., Zanin-Zhorov, A., Cohen, S., Cohen, I.R., and Zipori, D. (2007). Toll-like receptors and their ligands control mesenchymal stem cell functions. *Blood* 109, 1422–1432.
- Pradier, A., Passweg, J., Villard, J., and Kindler, V. (2011). Human bone marrow stromal cells and skin fibroblasts inhibit natural killer cell proliferation and cytotoxic activity. *Cell Transplant.* 20, 681–691.
- Prockop, D.J., and Oh, J.Y. (2012). Mesenchymal stem/stromal cells (MSCs): role as guardians of inflammation. *Mol. Ther.* 20, 14–20.
- Rajagopalan, S. (2014). HLA-G-mediated NK cell senescence promotes vascular remodeling: implications for reproduction. *Cell. Mol. Immunol.* 11, 460–466.
- Rajagopalan, S., and Long, E.O. (2012). Cellular senescence induced by CD158d reprograms natural killer cells to promote vascular remodeling. *Proc. Natl. Acad. Sci. USA* 109, 20596–20601.
- Scheller, J., Chalaris, A., Schmidt-Arras, D., and Rose-John, S. (2011). The pro- and anti-inflammatory properties of the cytokine interleukin-6. *Biochim. Biophys. Acta* 1813, 878–888.
- Spaggiari, G.M., Capobianco, A., Becchetti, S., Mingari, M.C., and Moretta, L. (2006). Mesenchymal stem cell-natural killer cell interactions: evidence that activated NK cells are capable of killing MSCs, whereas MSCs can inhibit IL-2-induced NK-cell proliferation. *Blood* 107, 1484–1490.
- Spaggiari, G.M., Capobianco, A., Abdelrazik, H., Becchetti, F., Mingari, M.C., and Moretta, L. (2008). Mesenchymal stem cells inhibit natural killer-cell proliferation, cytotoxicity, and cytokine production: role of indoleamine 2,3-dioxygenase and prostaglandin E2. *Blood* 111, 1327–1333.
- Stagg, J. (2007). Immune regulation by mesenchymal stem cells: two sides to the coin. *Tissue Antigens* 69, 1–9.
- Thomas, H., Jager, M., Mael, K., Brandau, S., Lask, S., and Flohe, S.B. (2014). Interaction with mesenchymal stem cells provokes natural killer cells for enhanced IL-12/IL-18-induced interferon-gamma secretion. *Mediators Inflamm.* 2014, 143463.
- Vivier, E., Tomasello, E., Baratin, M., Walzer, T., and Ugolini, S. (2008). Functions of natural killer cells. *Nat. Immunol.* 9, 503–510.
- Wang, Y., Chen, X., Cao, W., and Shi, Y. (2014). Plasticity of mesenchymal stem cells in immunomodulation: pathological and therapeutic implications. *Nat. Immunol.* 15, 1009–1016.
- Waterman, R.S., Tomchuck, S.L., Henkle, S.L., and Betancourt, A.M. (2010). A new mesenchymal stem cell (MSC) paradigm: polarization into a pro-inflammatory MSC1 or an immunosuppressive MSC2 phenotype. *PLoS One* 5, e10088.
- Wu, X., Jin, L.P., Yuan, M.M., Zhu, Y., Wang, M.Y., and Li, D.J. (2005). Human first-trimester trophoblast cells recruit CD56bright. *J. Immunol.* 175, 61–68.
- Wyles, C.C., Houdek, M.T., Crespo-Diaz, R.J., Norambuena, G.A., Stalboerger, P.G., Terzic, A., Behfar, A., and Sierra, R.J. (2015). Adipose-derived mesenchymal stem cells are phenotypically superior for regeneration in the setting of osteonecrosis of the femoral head. *Clin. Orthop. Relat. Res.* 473, 3080–3090.
- Zhang, X.L., Topley, N., Ito, T., and Phillips, A. (2005). Interleukin-6 regulation of transforming growth factor (TGF)-beta receptor compartmentalization and turnover enhances TGF-beta1 signaling. *J. Biol. Chem.* 280, 12239–12245.